Blind Prediction Challenge for Bonded Aircraft T-Joint Failure

G. Renaud[1*] and J. Finlay[2]

[1] Aerospace Research Centre, National Research Council of Canada, Ottawa, Canada,
[2] Aerospace Systems, National Research Council, Washington, DC, USA

* *Corresponding author (guillaume.renaud@nrc-cnrc.gc.ca)*

Keywords: *carbon-fibre-reinforced polymer; bonded joints; failure prediction; finite element analysis; cohesive zone modelling*

1. Abstract

This paper provides a high-level overview of an international blind prediction challenge for bonded composite T-joints, organized by Five Eyes Science and Technology (FVEY S&T). The goal of this challenge was to assess capabilities in modelling progressive damage in a generic bonded composite T-joint under three load cases and various defect scenarios. A high-level summary of the modelling assumptions and approaches employed by 13 participants is presented, along with normalized comparisons between the blind predictions and the test results. Key observations are discussed with respect to parameter selection, cohesive zone interface placement, intralaminar and interlaminar damage modelling, discretization, analysis efficiency, prediction accuracy, and identified best practices.

2. Introduction

Carbon fibre-reinforced polymer (CFRP) composite materials are widely used in modern aircraft structures due to their high specific strength and stiffness, resistance to corrosion, and extended fatigue life. Adhesively bonded composite joints offer advantages in primary airframe applications, as they eliminate the need for mechanical fasteners, reduce stress concentrations, and improve damage tolerance while decreasing manufacturing and assembly costs.

Despite these advantages, the certification of bonded composite joints remains challenging. Regulatory guidance requires demonstration of structural integrity, yet the internal state of adhesive bonds is difficult to assess, and failure mechanisms in bonded CFRP structures differ significantly from those in conventional metallic airframes. As the industry moves toward certification approaches that are less reliant on extensive experimental test campaigns, physics-based predictive modelling is becoming increasingly important.

Finite element analysis using progressive damage models has emerged as the primary method for simulating failure in bonded composite structures. However, the field lacks consensus on the most accurate and efficient modelling strategies for complex joint geometries and loading conditions. Key questions include the appropriate level of laminate discretization, the placement and parameterization of cohesive zone models (CZM) for adhesive disbonding and delamination, the use of intralaminar damage models, and trade-offs between model fidelity and computational cost.

To address these questions, the Five Eyes Science and Technology organization (FVEY S&T), formerly known as The Technical Cooperation Program (TTCP), launched a blind analysis challenge. This challenge invited research teams from Canada, the United Kingdom (UK), and the United States (USA) to blindly predict the failure of a representative bonded composite T-joint under multiple loading and defect conditions. The challenge was designed to assess how well modelling approaches meet the key requirements of an ideal progressive damage and failure analysis: accurate stiffness representation, correct failure modes and locations prediction, accurate or conservative peak load prediction, computational efficiency, and scalability to large assemblies.

3. Challenge Overview

First, participants were provided with a set of data including material characterization, test article geometry, ply stacking sequences, as well as boundary and loading conditions. Then, participants independently developed analysis models and submitted blind predictions of the load-displacement response, ultimate load, displacement at failure, damage locations and, if available, damage progression. Not all test cases had to be addressed. Finally, FVEY S&T released the experimental test results. Participants were then invited to compare their blind predictions with the experimental data and recalibrate their models if desired.

Thirteen individual or team participants submitted predictions. Each participant was assigned a label, A through M, for this summary paper. Table 1 lists the participants and their organizations.

Table 1. Participant organizations.

Label	Organization(s)	Country
A [1]	The Aerospace Corporation	USA
B [2]	National Research Council, Air Force Research Laboratory and Booz Allen Hamilton	USA
C	Air Force Research Laboratory	USA
D [3]	Global Engineering and Materials and Lockheed Martin Corporation	USA
E [4]	Imperial College London	UK
F [5]	National Composites Centre and University of Bristol	UK
G [6]	National Research Council of Canada	Canada
H [7]	National Research Council of Canada	Canada
I [8]	National Research Council of Canada and Carleton University	Canada
J [9]	Texas A & M University (TAMU)	USA
K [10]	University of Alabama	USA
L	University of Texas at Arlington	USA
M [11]	University of Texas at Arlington and Arizona State University	USA

3.1. Input Data Provided to Participants

Participants were provided with the following information prior to submitting their blind predictions:

- T-joint geometry, including nominal dimensions and ply stacking sequences. Cure cycle details were also provided.

- Mechanical properties for the CFRP lamina and properties for the film adhesive. Properties included elastic moduli (tension and compression), strengths, and fracture toughness determined from double cantilever beam (DCB), end notch flexure (ENF), and mixed mode bending (MMB) tests for both non-pre-cracked (NPC) and pre-cracked (PC) conditions. These fracture tests were performed on unidirectional coupons with and without adhesive, as well as coupons with a nonstandard layup with adhesive intended to be representative of the T-joint bondline and adjacent plies.
- Test setup configurations, boundary conditions, and loading descriptions for each test case.
- Initial stiffness data to allow participants to perform a sanity check of their model setup.

4. Test Article and Test Conditions

The test specimen was an adhesively bonded composite T-joint, representative of the connection between a stiffener and a wing skin panel in a composite airframe. As illustrated in Figure 1, the joint consisted of five structural components: a skin laminate, an adhesive film, a spar cap, two C-shaped channel laminates, and a noodle filling the gap between the C-channels and the spar cap. All composite components were made of IM7/5320-1 carbon/epoxy unidirectional prepreg tape. The two C-channels, noodle, and spar cap were co-cured to form the stiffener assembly. The stiffener was then adhesively bonded to the skin using FM309-1M film in a secondary bonding operation. The noodle was formed from a rolled unidirectional lamina of the same material.

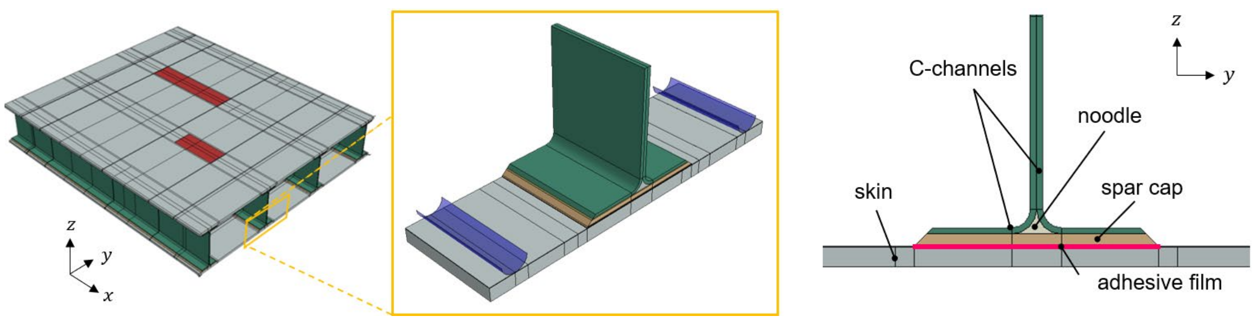

Figure 1. T-joint representing a repeat unit of a wing box and schematic cross-section of the bonded composite T-joint specimen.

4.1. Loading Conditions and Defect Configurations

Three loading conditions were investigated: T-Pull, Side-Bend, and Mixed-Shear. In the T-Pull test, a vertical load was applied to the web while the skin was constrained by two rollers. In the Side-Bend test, a lateral load was applied to the web by a roller, while two supporting rollers and contact with a wall prevented rigid-body motions. In the Mixed-Shear test, a vertical load was applied to a loading fork, resulting in a mixed shear stress state in the bondline.

Three configurations of the T-Pull and Side-Bend specimens were tested: a pristine (no defect) configuration and two configurations with pre-induced artificial defects. Defects were introduced by placing PTFE (Teflon) film inserts between the adhesive layer and the skin laminate prior to bonding, preventing bond formation in the insert region. Two defect types were considered: tip and throat defects. In the Mixed-Shear test, the only specimen configuration included a large

Teflon insert causing an initial disbond of approximately half the bondline. All together, a total of seven test cases were investigated. The defect and loading conditions are illustrated in Figure 2.

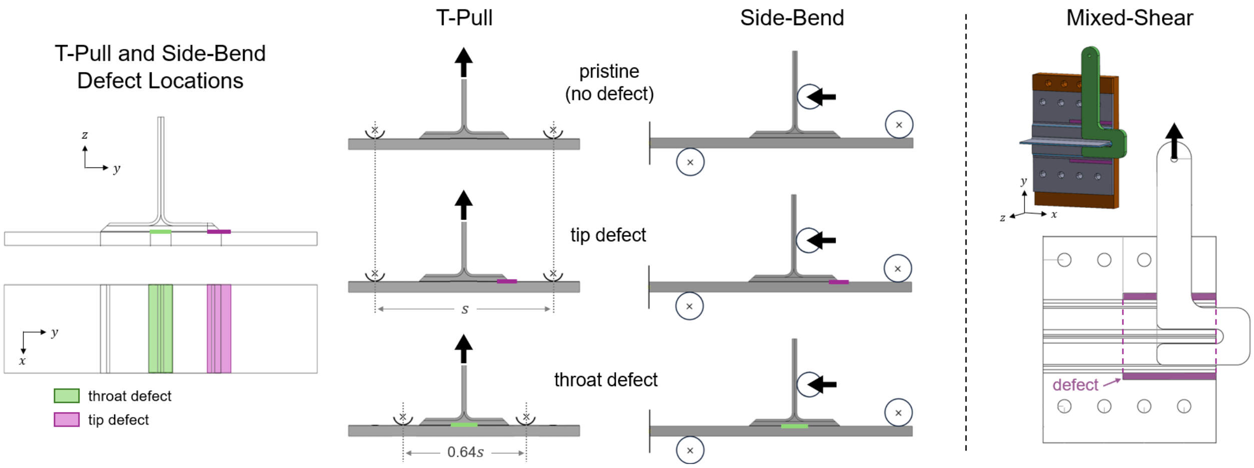

Figure 2. Defect and loading configurations.

5. Overview of Experimental Results

5.1. T-Pull Results

Experimental results for the T-Pull test showed an initial linear load-displacement response, followed by an abrupt failure in all configurations. The pristine (no defect) and tip defect cases exhibited low scatter in stiffness and strength, consistent with a single dominant failure mechanism: adhesive cohesive failure or adhesive-skin delamination initiating from the bondline edges. The tip defect reduced both stiffness and strength relative to the pristine case. The throat defect configuration showed noticeably higher stiffness than the other two cases, attributable to the shorter roller span (Figure 2), which increased the bending stiffness of the supported assembly. Throat defect specimens exhibited significantly higher strength scatter than the pristine and tip defect cases. Two competing failure modes were observed in the throat defect specimens: failure initiating in the adhesive bond region (similar to the pristine and tip defect cases), or failure developing in the noodle region with horizontal delamination beneath the noodle and vertical fracture in the web. No correlation was observed between failure location and ultimate strength; specimens that failed at either location covered a similar range of loads. The T-Pull experimental load-displacement curves are provided in Figure 3.

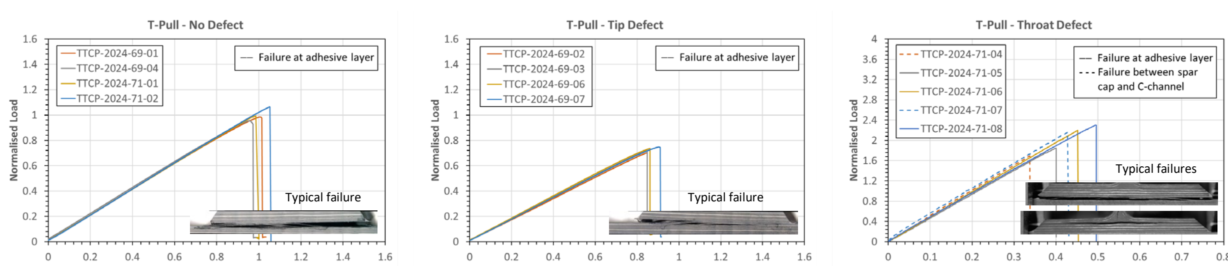

Figure 3. T-Pull experimental load-displacement curves.

5.2. Side-Bend Results

Side-Bend experimental results show that all specimens, regardless of the presence or location of a defect, can be separated into two clusters of ultimate loads, with the higher cluster approximately 50% higher than the lower one. Subsequent investigation revealed that this clustering correlated with the parent panel from which specimens were cut (Panel 69 and Panel 71). Within each panel batch, specimens of different defect types showed no significant difference in ultimate load or failure mechanism. Although both panels were manufactured identically, this observation suggests that the scatter in Side-Bend results reflects manufacturing variability rather than a defect-driven mechanical response. Failure in all Side-Bend specimens occurred through delamination within the C-channel and interfacial decohesion between the C-channel and the noodle, independently of the defect type. These two failure modes occurred almost simultaneously in all cases, consistent with the two damage events being energetically coupled at the noodle radius. The adhesive bondline was not involved in the failure process. For this reason, all Side-Bend experimental results were combined for this summary paper. Following the primary load drop, all specimens exhibited a residual load plateau similar across all defect conditions and both panel batches.

5.3. Mixed-Shear Results

The Mixed-Shear experimental results exhibited characteristics that warrant further investigation. Test results showed high scatter in ultimate load, and at least two distinct failure behaviours were identified, suggesting that more than one dominant failure mechanism was active in this configuration. A preliminary indication of two strength clusters was observed, with an apparent correlation with the parent panel, Panel 69 specimens tending toward higher strength. This is the inverse of the panel correlation observed in Side-Bend.

The Side-Bend and Mixed-Shear load-displacement curves are provided in Figure 4, along with examples of failure for these configurations.

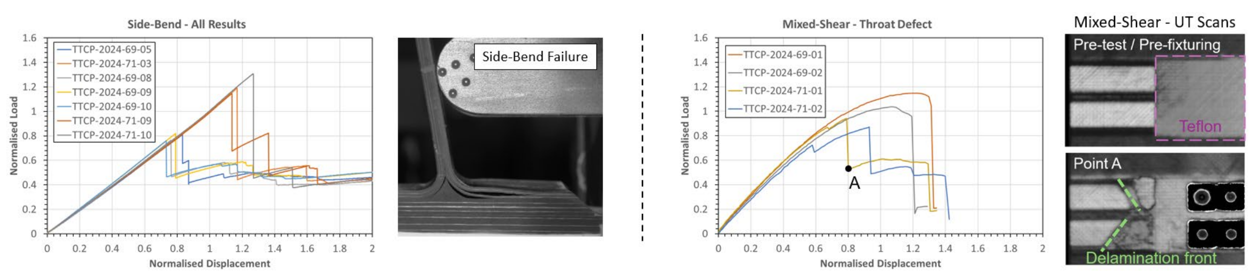

Figure 4. Side-Bend and Mixed-Shear results.

6. Overview of Blind Submissions

A total of 13 participants submitted predictions, with 11 presenting their work at the AIAA SciTech 2026 Forum. The number of individual submissions per participant ranged from one to six, reflecting different modelling strategies or coverage of different test cases. Not all participants addressed all seven test cases: the T-Pull cases were covered by all 13 participants, while coverage of Side-Bend and Mixed-Shear cases was more limited. Detailed submission information for 11 of the participants can be found in the individual papers presented at SciTech 2026 [1-11]. The contributions of participants C and L are only represented by the blind submission data.

6.1. Summary of Modelling Approaches

The large majority of participants used Abaqus with either implicit or explicit solvers, with or without in-house user material subroutines. One participant (J) used a custom MATLAB framework, achieving run times of seconds per case. Table 2 summarizes high-level characteristics of the modelling approaches taken by the participants. Acronyms are defined in [1-11]

Table 2. Summary of modelling approaches.

Submission	Intralaminar Damage	Interlaminar Damage	Laminate Resolution
A [1]	First-ply failure criteria (Max Stress, Tsai-Wu, Christensen, Puck 2D)	Tong (adh); VCCT at defect tips (no CZM); interlaminar tension/shear criterion (added post-blind)	Med-High (skin ply-by-ply; sub-laminate elsewhere)
B [2]	None or matrix cracking via CZM strips (variants)	Standard CZM - adh/skin + 3 skin ply interfaces; single smeared interface (low-fidelity variant)	Med (outer 4 plies explicit)
C	None	Cohesive contact (not cohesive elements) - spar/skin + spar web/cap including noodle	Low (homogenized continuum shell)
D [3]	LaRC04 + exponential CDM + Ramberg-Osgood shear nonlinear	Standard Abaqus bilinear CZM - adh/skin interface + top 10 skin ply interfaces + bottom 7 spar cap ply interfaces	Med-High (top 10 skin plies explicit)
E [4]	Modified LaRC05 progressive damage	CZM elements (adhesive) + cohesive contact (interlaminar); B-K criterion	High (ply-by-ply) solid shell and C3D8R variant
F [5]	None	Custom VUMAT CZM - Disb + Delam (compression on Mode II; displacement-based)	High (ply-by-ply)
G [6]	None	Standard CZM - Disb + Delam (T-Pull/SB); VCCT for skin/cap disb. + CZM for cap delam. (Mixed-Shear, hybrid approach)	Med (half-width blind; unit-width post)
H [7]	LaRC05 onset only (no degradation)	Standard CZM - Disb + Delam	High (ply-by-ply solid elements)
I [8]	Enhanced LaRC05 full progressive	Standard CZM (delam. in skin, spar, C-channel; disb. at C-channel/noodle and C-channel/spar; cohesion failure in adhesive) + intralaminar CZM for discrete matrix cracking; two fracture energy sets	High (ply-by-ply)
J [9]	GraFEA (critical strain threshold)	LDM strain-degradation decohesion - thermodynamically consistent	Low (homogenized beam layers)
K [10]	None	Standard Abaqus bilinear CZM	Med (0.1 mm slice; through-thickness)
L	Ply cracks	Multiple CZM interfaces: stiffener/skin + ply 1/2 + ply 2/3 (at minimum)	Med–High (≥3 skin plies explicit)
M [11]	2D Enhanced Schapery Theory (EST) - fiber breaking, micro, macro matrix cracking	Standard Abaqus CZM (COH3D8 + cohesive contact) - Disb + Delam (blind); C-channel/noodle interface added post-test (SB only)	Med (continuum shell SC8R; 0.7–3 mm graded)

The most common interlaminar failure approach was the built-in Abaqus cohesive zone modelling (CZM) with the bilinear traction-separation law and the B-K mixed-mode damage evolution (except for J, who used a power law criterion). Intralaminar failure models ranged from none through initiation-only criteria to full progressive damage models. One participant (A) used a linear elastic approach with strength-based failure criteria and the virtual crack closure technique (VCCT) rather than CZM. This participant submitted damage initiation loads based on first-ply failure criteria, not predicted ultimate loads. Laminate discretization ranged from fully homogenized through sub-laminate homogenization with select ply-by-ply discretization to full ply-by-ply resolution. One participant (F) included a cool-down simulation to account for thermal residual stresses and modelled the adhesive as an elastoplastic material. Computational costs spanned six orders of magnitude, from seconds per case (J) to thousands of CPU-hours (M).

7. Comparison of Blind Predictions with Experimental Results

Across all seven test cases, approximately one third of blind predictions fell within ±15% of the average experimental results. Performance varied significantly by load case: T-Pull predictions were the most accurate overall, with Side-Bend predictions predominantly unconservative, and Mixed-Shear predictions clustered within roughly ±40% of the experimental average.

The primary metric for comparing blind predictions in this paper is the relative error in predicted peak (ultimate) load with respect to the average experimental result. A positive error indicates an unconservative prediction (overprediction of strength); a negative error indicates a conservative prediction. Force and displacement values were normalized. Blind predictions errors are summarized in Table 3 and selected cases are shown graphically in Figure 5. Post-test calibration results, which sometimes substantially improved simulation accuracy (e.g. J), are not presented.

7.1. T-Pull Results

Across all participants using CZM-based approaches, T-Pull strength predictions were generally reasonable, with errors in the range of 0% to 35% for most submissions. Stiffness was generally well-predicted across all participants, confirming that the boundary conditions and the model setup were generally appropriate. The best overall performance in terms of accuracy and conservativeness was observed for the No Defect and Throat Defect cases, but some of the best-performing submissions also achieved strong results for the Tip Defect case (participants E and F, both within 5%), suggesting that explicit modelling of near-bondline skin ply interfaces, which captures the multi-interfacial delamination, can be a key differentiator for this configuration.

7.2. Side-Bend Results

The spread in accuracy was significant for Side-Bend predictions, with errors ranging from near-zero to several hundred percent. The large majority of Side-Bend blind predictions overestimated the strength, reflecting the absence of damage modeling in the noodle region in many models. This is the inverse of the conservative bias observed for T-Pull, and underscores that unconservatism in blind predictions is load-case specific rather than a general property of the methods used. The most significant driver of prediction error was CZM placement: participants who omitted the C-channel/noodle interface predicted failure at the wrong location and grossly overpredicted load. Participant I, who included this interface from the outset, achieved conservative errors of 19-20%.

7.3. Mixed-Shear Results

The Mixed-Shear case was addressed by a subset of participants. Predictions clustered within roughly ±40% of the average experimental result, a spread reflecting variability in adhesive fracture energy selection rather than fundamental modelling disagreements on failure modes or locations. Predictions that focused on adhesive bondline failure achieved the best accuracy, consistent with the finding that adhesive-dominated failure was well-characterized by the provided DCB/ENF fracture data. The asymmetric damage front associated with the predominantly Mode III loading was captured by the full 3D models used for this case. Participant M achieved a blind prediction error of 18% for this case, with the predicted V-shaped delamination front and progressive damage growth history in close agreement with ultrasonic scans (Figure 4).

Table 3. Summary of blind prediction errors. Bold values indicate conservative predictions

Submission	T-Pull			Side-Bend			Mixed-Shear
	Pristine	Tip	Throat	Pristine	Tip	Throat	
A [1]*							
B [2]**							
C	**34%**	**23%**	**35%**	**48%**	**48%**	**48%**	
D [3]	7%	26%	10%	20%	20%	20%	41%
E [4]	**16%**	0%	4%	**4%**	**4%**	**4%**	30%
F [5]	**17%**	**5%**	**12%**	**14%**	**13%**	**14%**	
G [6]	**2%**	24%	8%	53%	52%	53%	**30%**
H [7]	3%	19%	20%	77%	77%	94%	
I [8]	**22%**	**24%**	**24%**	**19%**	**20%**	**20%**	
J [9]	20%	38%	47%	359%	353%	209%	**36%**
K [10]	4%	28%	19%	215%	211%	195%	2%
L	**12%**	10%	**6%**				
M [11]	12%	11%	13%	484%	370%	388%	18%

* Participant A submitted multiple failure criteria rather than predicted failure loads
** Participant B's submissions, co-author of this paper, were not truly blind (not included)

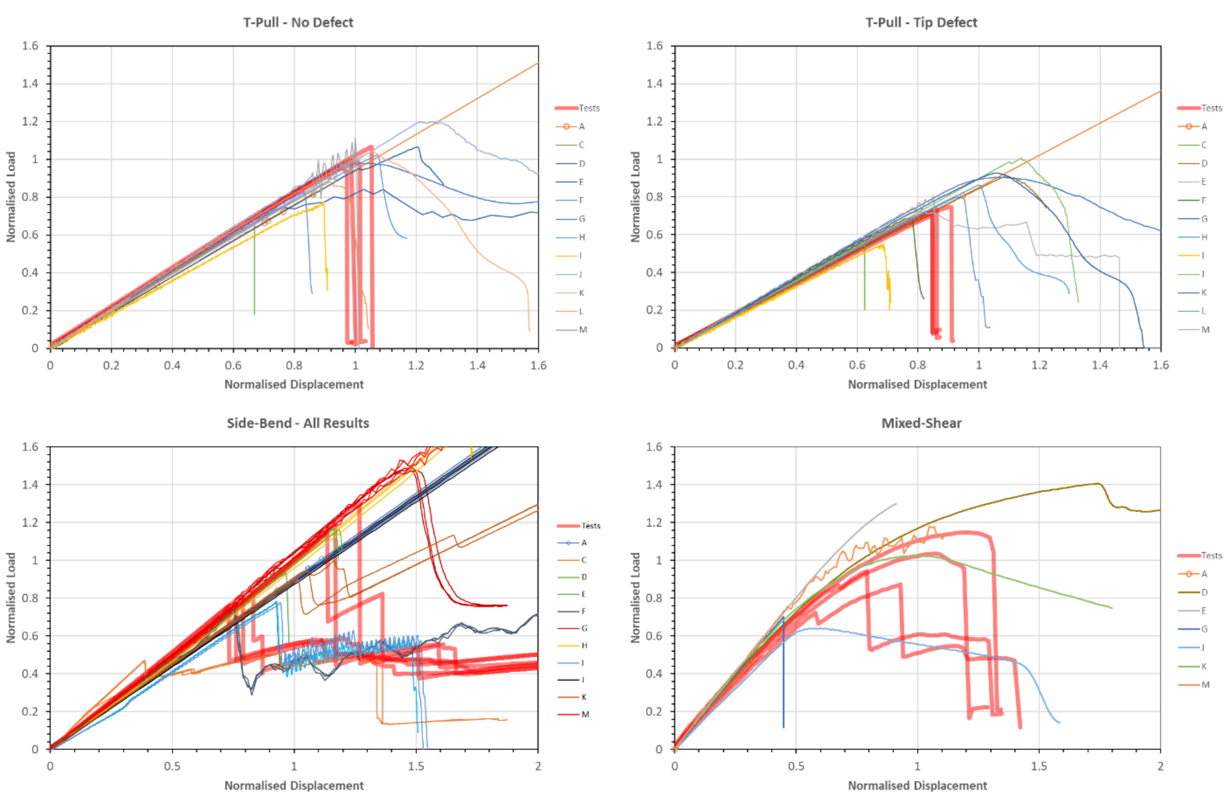

Figure 5. Typical comparisons between blind prediction and experimental results.

8. General Observations and Recommendations

Some observations about the blind predictions include the following:

- The selection of fracture energy values (NPC vs. PC, unidirectional vs. representative layup) varied significantly among participants.
- The computational cost spanned six orders of magnitude (seconds to thousands of CPU-hours).
- Method selection dominates over hardware. Medium-fidelity models achieved accuracy comparable to ply-by-ply models at a fraction of the cost.
- The adhesive material was significantly tougher than the composite laminate. Under mixed-mode loading, crack paths tended to migrate from the adhesive bondline into the laminate. Models that do not account for this migration were at risk of predicting incorrect failure modes.

A systematic approach to fracture energy selection, informed by the nature of crack initiation at each interface, is recommended. Further, a preliminary elastic (no-damage) analysis is also recommended as a standard first step before any progressive damage simulation. Stress concentration patterns and principal stress directions in the elastic structure provide reliable guidance for CZM placement and identification of critical regions - the single most impactful modelling decision in this challenge. Several participants who missed key failure locations would likely have identified them through such a preliminary analysis.

Validation of CZM fracture energy parameters through coupon-level simulation of the provided DCB and ENF tests, rather than direct use of tabulated values, is recommended good practice. This validation is especially important when using element sizes large enough to efficiently simulate structures. Participants who explicitly verified their CZM implementation against coupon data achieved consistently reliable adhesive-dominated predictions. This step also serves as a check on cohesive strength, penalty stiffness selection, and mixed-mode interaction law behaviour.

9. Conclusions

This paper has presented the results of a blind prediction challenge for a bonded composite T-joint under T-Pull, Side-Bend, and Mixed-Shear loading. The following principal conclusions are drawn:

- T-Pull failure loads were generally predicted within 35% by most CZM-based participants, demonstrating that current modelling approaches have reasonable predictive capability for delamination-dominated failure. Stiffness was consistently well-predicted across all approaches.
- Simultaneous delamination at the adhesive bondline and adjacent skin ply interfaces governed the T-Pull tip defect case. Single-interface CZM models that do not include near-bondline skin-ply interfaces overpredicted this configuration strength by approximately 19-28%.
- Side-Bend predictions showed much greater variability than T-Pull. CZM placement, specifically the inclusion of damageable interfaces within the C-channel laminates and at the C-channel/noodle interface, was the determining factor for capturing the correct failure mode and achieving accurate strength predictions.

Post-test investigation revealed that the as-manufactured adhesive bondline thickness was substantially thinner than the nominal value, a discrepancy that may have influenced strength predictions. As future work, it is planned to conduct new DCB, ENF, and MMB tests with controlled adhesive thickness to generate input parameters more representative of the tested T-joint configurations. Participants will have the opportunity to revise their models and assess whether more representative material data affect the accuracy of their predictions.

10. Acknowledgements

The authors gratefully acknowledge the contributions of all challenge participants and the support of the Five Eyes Science and Technology (FVEY S&T) organization. Material characterization tests were conducted by the Air Force Research Laboratory (AFRL). The challenge was coordinated under the FVEY S&T collaborative project "Benchmarking and Development of Digital Tools for Composite Structural Analysis."

11. References

[1] B. Soltz, U. Agwu, M. Ghabbour, K. Moore, M. Wang and V.K. Goyal, "Comparison of Composite Failure Predictions and Experimental Results in a Blind Study", AIAA SciTech Forum, Orlando, January 2026.

[2] J. Finlay, S.B. Clay and N. Loomis, "An Investigation of Modeling Strategies for the Structural Response and Failure of Composite T-Joints", AIAA SciTech Forum, Orlando, January 2026.

[3] A. Karuppiah, R. Li, V.K. Goyal and J. Lua, "High-Fidelity Progressive Damage Predictions of Composite T-Joints with Seeded Defects in CB^{2}ATA", AIAA SciTech Forum, Orlando, January 2026.

[4] M. Miranda, R. Li and S.T. Pinho, "Behaviour of Adhesively Bonded Composite Stiffeners: A Blind Prediction Exercise", AIAA SciTech Forum, Orlando, January 2026.

[5] S. Green, S.R. Hallett, G. Allegri and H. Wright, "Failure of Adhesively Bonded Composite Stiffeners: a Blind Analysis Challenge", AIAA SciTech Forum, Orlando, January 2026.

[6] G. Li, "Application of Cohesive Elements to Predict Lead Failure Behaviors in Bonded Composite T-Joints under Two Load Cases", AIAA SciTech Forum, Orlando, January 2026.

[7] H.H. Liu and G. Qi, "Progressive Damage and Failure Analysis of Composite Laminate Structure", AIAA SciTech Forum, Orlando, January 2026.

[8] P. Shabani, L. Li and J. Laliberte, "Progressive Failure Analysis of Bonded Composite Specimens Under T-Pull and Side-Bend Loadings Using Integrated Discrete-Continuum Damage Models", AIAA SciTech Forum, Orlando, January 2026.

[9] S. Hari, P. Kumar, A.R. Srinivasa and J.N. Reddy, "Layerwise Decohesion Model: A Computationally Efficient Delamination Model for T-Shaped Composite Structures Under Pull and Side-Bend Loading", AIAA SciTech Forum, Orlando, January 2026.

[10] B. Kar, S. Aditya and S. Roy, "TTCP Blind Analysis Challenge: Simulation of T-Pull Tests using the Power Law and B-K Mixed-Mode Progressive Failure Criteria in ABAQUS", AIAA SciTech Forum, Orlando, January 2026.

[11] S. Lin and A. Waas, "Progressive Damage and Failure Predictions of T-Pull and Side Bend Tests of Composite Joints", AIAA SciTech Forum, Orlando, January 2026.